2.5A

A STUDY OF THE OKLAHOMA CITY URBAN HEAT ISLAND USING GROUND MEASUREMENTS AND REMOTE SENSING

* Michael J. Brown[1], Austin Ivey[1], Timothy N. McPherson[1], David Boswell[1], Eric R. Pardyjak[2]

[1]Los Alamos National Laboratory, Los Alamos, New Mexico
[2]Department of Mechanical Engineering, University of Utah, Salt Lake City, Utah

1. INTRODUCTION

Measurements of temperature and position were collected during the night from an instrumented van on routes through Oklahoma City and the rural outskirts. The measurements were taken as part of the Joint URBAN 2003 Tracer Field Experiment conducted in Oklahoma City from June 29, 2003 to July 30, 2003 (Allwine et al., 2004). The instrumented van was driven over four primary routes that included legs from the downtown core to four different "rural" areas. Each route went through residential areas and most often went by a line of permanently fixed temperature probes (Allwine et al., 2004) for cross-checking purposes. Each route took from 20 to 40 minutes to complete. Based on seven nights of data, initial analyses indicate that there was a temperature difference of 0.5-6.5 °C between the urban core and nearby "rural" areas. Analyses also suggest that there were significant fine scale temperature differences over distances of tens of meters within the city and in the nearby rural areas. The temperature measurements that were collected are intended to supplement the meteorological measurements taken during the Joint URBAN 2003 Field Experiment, to assess the importance of the urban heat island phenomenon in Oklahoma City, and to test new urban canopy parameterizations that have been developed for regional scale meteorological codes (e.g., Chin et al., 2000; Holt and Shi, 2004).

In addition to the ground measurements, skin temperature measurements were also analyzed from remotely sensed images taken from the Earth Observing System's Advanced Spaceborne Thermal Emission and Reflection Radiometer (ASTER). A surface kinetic temperature thermal infrared image captured by the ASTER of the Oklahoma City area on July 21, 2001 was analyzed within ESRI's ArcGIS 8.3 to correlate variations in temperature with land use type. Analysis of this imagery suggests distinct variations in temperature across different land use categories. Through the use of remotely sensed imagery we hope to better understand the development of the urban heat island analysis.

**Corresponding author address*: Michael J. Brown, Group D-4, MS F604, Los Alamos National Laboratory, Los Alamos, NM 87545: email: mbrown@lanl.gov.

2. GROUND-BASED MEASUREMENTS

2.1 Instrumentation and Software

A Chevrolet Astro van was instrumented with a thermistor probe and a GPS unit for obtaining temperature and vehicle position, respectively. The thermistor was mounted on a 1.5 cm diameter PVC sting and the GPS unit was taped to the roof. The sting was affixed to the van on the rear bumper with the temperature probe approximately 2.75 m above the ground (Fig. 1).

The temperature data were taken using a YSI 4600S (Transfer Standard) Precision Thermometer in conjunction with an "in-house" University of Utah Matlab data acquisition program run on a PC laptop. Time and temperature data were acquired through a serial (RS-232) interface at a rate of one sample every 524 milliseconds. The time constant of the YSI 4600S is one second in an oil bath and five to ten seconds in air, the resolution is 0.01 °C, and the accuracy is ± 0.025°C from 0° to 50°C. Our unit was calibrated at five points with a YSI 052 Bird Cage Air Probe and has certified NIST traceability.

The van position was obtained with a DeLorme Earthmate GPS. Position, time, and velocity data were saved to a file via a serial connection interface using DeLorme's Topo U.S.A. 2.0 software on a second PC laptop. Satellite accessibility limited the data rate of the GPS system and caused it to be slightly irregular, ranging between 0.25 and 1 Hz. The horizontal accuracy of the GPS varied between 10 and 15 meters while moving. The speed range over which the van traveled was from 0 to 35 mph with periods of highway driving at around 65 mph on return routes.

2.2 Route Description

Routes were driven in four directions from the central business district in Oklahoma City. The routes were designed to take approximately a half hour to traverse from urban to rural areas to minimize the effects of temperature changes in the calculation of the urban heat island intensity. The routes covered the northeastern, eastern, southwestern and south-eastern urban to rural transitions and data were collected on both the outbound and return trips. The routes were chosen to contain many landuse types, including the central business district, warehouse districts, strip malls, low and high density residential areas, and various types of open space rural areas.

A secondary goal in the route design was to pass an array of telephone-pole-mounted temperature sensors (HOBOS) by a team of researchers from Pacific Northwest National Laboratory (Allwine et al., 2004) for cross-check purposes.

Every route included a trip through the downtown core. The buildings in this area are typically a few stories to tens of stories high and cover a relatively small area of about ten square blocks. In order to compute an urban-rural temperature difference, our routes took us to four different open space areas that were deemed representative of rural conditions. On our first route, the open space area was the undeveloped area surrounding the Oklahoma City Will Rogers Airport. The second open space area was farther out of the city to the southeast and included agricultural areas and a large lake called Stanley Draper. The third major route was from the city center out to the park containing the zoo and Northeast Lake in the northeast section of Oklahoma City. The fourth route was due east from the city center and traversed through high density to low density residential areas with the final goal an area of undeveloped open space interspersed with some small industrial facilities. The first route is referred to as the Airport route; the second route is the Lake Draper route; the third route is the NE Lake route; and the fourth route is the E. Rural route. A fifth route including a residential neighborhood north of the downtown urban core was often performed as this was our home base. The elevation change over these routes was minimal, however, there were small hills and valleys interspersed in the rural areas.

Table 1 – Experiment Route Descriptions

Expt No.	Date	Time (CDT)	Route
$1A_1$	JULY 14	15:42-16:09	Downtown – Residential
$1B_1$	JULY 14	20:01-20:49	Residential – E. Rural
$2A_1$	JULY 15	23:20-23:59	Residential - Airport
$2B_1$	JULY 16	01:37-02:20	Downtown - Residential
$3A_1$	JULY 17	21:29-22:02	Downtown - NE Lake
$3A_2$	JULY 17	22:02-22:17	NE Lake - Downtown
$3B_1$	JULY 17	22:17-22:35	Downtown - Airport
$3B_2$	JULY 17	22:35-22:49	Airport - Downtown
$3C_1$	JULY 17	22:49-23:07	Downtown - NE Lake
$3C_2$	JULY 17	23:07-23:28	NE Lake - Downtown
$3D_1$	JULY 18	02:32-02:52	Downtown -Lake Draper
$3D_2$	JULY 18	02:52-03:18	Lake Draper -Downtown
$3E_1$	JULY 18	03:24-03:43	Downtown - Airport
$3E_2$	JULY 18	03:44-03:58	Airport - Downtown
$4A_1$	JULY 18	23:38-23:57	Downtown -Lake Draper
$4B_1$	JULY 19	02:01-02:17	Downtown - NE Lake
$4B_2$	JULY 19	02:17-02:32	NE Lake - Downtown
$5A_1$	JULY 19	23:20-23:51	Residential - Downtown
$5B_1$	JULY 19	23:51-23:59	Downtown – E. Rural
$5C_1$	JULY 20	02:32-02:40	Downtown- Residential
$5C_2$	JULY 20	02:42-02:54	Residential - Downtown
$6B_1$	JULY 21	22:54-23:15	Downtown –Lake Draper
$6B_2$	JULY 21	23:15-23:43	Lake Draper -Downtown
$6C_1$	JULY 21	23:43-23:55	Downtown - Industrial
$6C_2$	JULY 22	01:57-02:08	Industrial - Downtown
$6D_1$	JULY 22	02:08-02:31	Downtown - Airport
$6D_2$	JULY 22	02:31-02:45	Airport - Downtown
$6E_1$	JULY 22	02:45-02:51	Downtown - Residential
$7A_1$	JULY 25	22:21-22:26	Residential - Downtown
$7B_1$	JULY 25	22:26-22:38	Downtown – E. Rural
$7B_2$	JULY 25	22:38-22:47	E. Rural - Downtown
$7B_3$	JULY 25	22:47-22:56	Downtown – E. Rural
$7B_4$	JULY 25	22:56-23:06	E. Rural - Downtown
$7B_5$	JULY 25	23:06-23:16	Downtown – E. Rural
$7B_6$	JULY 25	23:16-23:25	E. Rural - Downtown
$7B_7$	JULY 25	23:25-23:34	Downtown – E. Rural
$7B_8$	JULY 25	23:34-23:44	E. Rural - Downtown
$7C_1$	JULY 25	23:47-23:55	Downtown - NE Lake
$7C_2$	JULY 26	00:34-00:48	NE Lake - Downtown
$7C_3$	JULY 26	00:48-01:06	Downtown - NE Lake
$7C_4$	JULY 26	01:06-01:20	NE Lake - Downtown
$7C_5$	JULY 26	01:20-01:35	Downtown - NE Lake
$7C_6$	JULY 26	01:35-01:48	NE Lake - Downtown
$8A_1$	JULY 27	01:57-02:24	Downtown - Airport
$8A_2$	JULY 27	02:24-02:38	Airport - Downtown
$8A_3$	JULY 27	02:38-02:59	Downtown - Airport
$8A_4$	JULY 27	02:59-03:12	Airport - Downtown

3. REMOTE SENSING

3.1 Methodology

We have utilized remotely-sensed thermal infrared imagery in order to better understand the nature of the development of the urban heat island in Oklahoma City. To accomplish this, NASA thermal infrared imagery was acquired via the Land Processes Distributed Active Archive Center (LPDAAC) for our study area and geographically projected using ArcGIS. Analyses were then completed using the Association of Central Oklahoma Governments (ACOG) land cover assessment for the Oklahoma City area to correlate land use types and skin temperature.

3.2 Instrumentation

The Advanced Spaceborne Thermal Emission and Reflection Radiometer (ASTER) is part of the Earth Observing System Terra suite of instruments launched in December 1999. ASTER instrumentation was designed and assembled by a consortium of public and private Japanese groups. ASTER is comprised of fourteen spectral sensors including visible near-infrared (VNIR), short-wave infrared (SWIR) and thermal infrared (TIR) sensors at 15, 30 and 90 meter resolution, respectively.

3.3 Imagery

For the purposes of our urban heat island study, ASTER surface kinetic temperature (AST_08) imagery was downloaded via the LPDAAC. The following description taken from the LPDAAC describes the process of generating the surface kinetic temperature imagery:

"*Surface kinetic temperature is determined by applying Planck's Law using the emissivity values from the Temperature-Emissivity Separation (TES) algorithm, which uses atmospherically corrected ASTER Surface Radiance (TIR) data. The TES algorithm first estimates emissivities in the TIR channels using the Normalized Emissivity Method (NEM). These estimates are used along with Kirchoff's Law to account for the land-leaving TIR radiance that is due to sky irradiance. That figure is subtracted from TIR radiance iteratively to estimate the emitted radiance from which temperature is calculated using the NEM module*."

Numerous surface kinetic temperature images were requested in order to increase the probability of obtaining an image that canvassed our entire study area. Raw images were downloaded for conversion into a readable GIS format. All EOS Terra ASTER imagery is prepared in HDF-EOS format as developed by the National Center for Super-computers. The HDF-EOS format applies standards for geolocation and technical data to the imagery. Since this type of file association is not recognized by ArcGIS, the images were converted to Geo-TIFF format using a tool developed by the EOS Core System Project Office.

4. RESULTS

4.1 Ground-based Measurements

The downtown-to-airport route was performed ten times during the Joint Urban experiment. Figure 1 shows temperature measurements obtained over this route between 10:17 and 10:49 pm (CDT) on July 17, 2003. As on other nights, the temperatures are warmest in the downtown area and are coolest in the fields around the airport. The residential and industrial/warehouse regions contain intermediate temperatures. During this route, the temperature difference between the urban core and the rural area is about 4.5°C. As shown in Table 2, the urban-rural ΔT for this route varied from 2°C to 4.5°C during the experiment. Also listed is the cloud cover as obtained from the OKC Airport and the wind speed from a rooftop sensor 1.5 km to the northwest of the downtown area. For measurements collected on the same night, the ΔT tends to decrease with time. Note that in our calculations of ΔT we are not using the minimum rural temperature and maximum urban temperature measured on the route, but rather we are using a rough estimate of spatially-averaged temperatures.

Table 2 – Urban-Rural Temp. Difference Downtown-Airport Route

Expt No.	Date	Time (CDT)	Cloud Cover	wind speed (m/s)	ΔT (C)
$3B_1$	7-17	22:17-22:35	CLR	3.0-4.0	**4.4**
$3B_2$	7-17	22:35-22:49	CLR	3.0-4.0	**3.9**
$3D_1$	7-18	03:24-03:43	CLR	4.5	**2.0**
$3D_2$	7-18	03:44-03:58	CLR	4.5	**1.8**
$6D_1$	7-22	02:08-02:31	CLR	3.5	**4.2**
$6D_2$	7-22	02:31-02:45	CLR	3.5	**2.5**
$8A_1$	7-27	01:57-02:24	CLR	5.0	**2.9**
$8A_2$	7-27	02:24-02:38	CLR	5.0	**2.1**
$8A_3$	7-27	02:38-02:59	CLR	5.0	**3.4**
$8A_4$	7-27	02:59-03:12	CLR	5.0	**2.6**

The downtown-to-NE Lake route was driven twelve times during the experiment. Figure 2 shows temperature measurements obtained over this route between 12:34 and 1:06 am (CDT) on July 26, 2003.

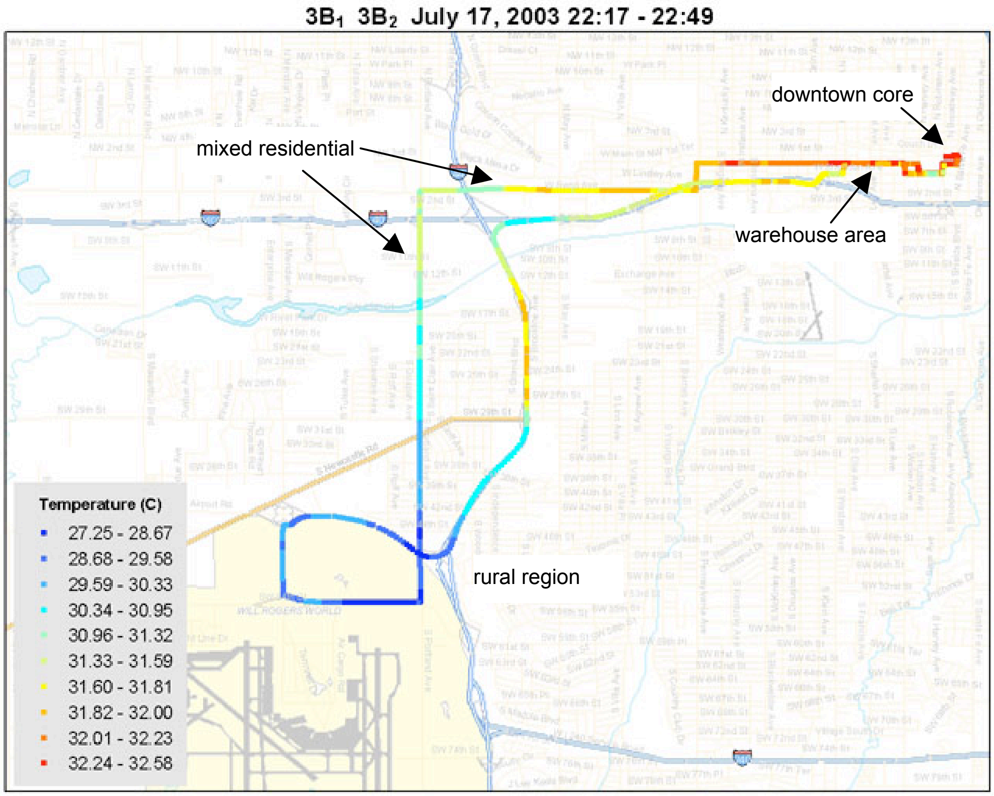

Figure 1. The downtown-to-airport route showing temperature measurements made at 2.5 m above ground level on the night of July 17, 2003.

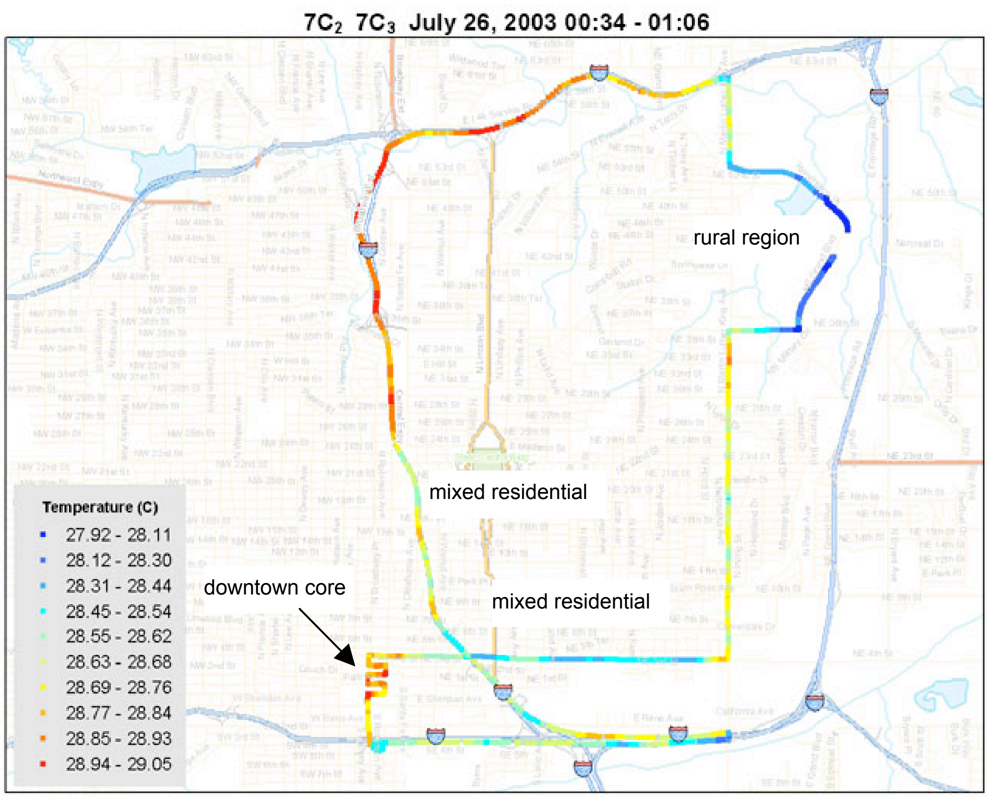

Figure 2. The downtown-to-NE Lake route showing temperature measurements made at 2.5 m above ground level in the early morning hours of July 26, 2003.

Surprisingly, this route did not always show the warmest temperatures in the downtown area, but often were along I-235 near the junction with I-44. These warm temperatures were consistent over different nights and times. During this route, the temperature difference between the urban core and the rural area near the zoo and NE Lake is about 0.8°C. As shown in Table 3, the urban-rural ΔT for this route varied from 0.5°C to 1°C during the experiment, with one 4°C outlier. This higher ΔT may have occurred due to lower wind speeds (3 m/s) and being earlier in the night (around 11 pm). The ΔT was large on this night for other routes as well. The trend of decreasing ΔT as it gets later in the night occurs on this route too.

Table 3 – Urban-Rural Temp. Difference Downtown-NE Lake Route

Expt No.	Date	Time (CDT)	Cloud Cover	wind speed (m/s)	ΔT (C)
$3C_1$	7-17	22:49-23:07	CLR	3.0-4.0	**4.1**
$4B_1$	7-19	02:01-02:17	CLR	4.0	**1.4**
$4B_2$	7-19	02:17-02:32	CLR	4.0	**0.8**
$7C_1$	7-25	23:47-23:55	CLR	6.0	**1.1**
$7C_2$	7-26	00:34-00:48	CLR	6.0	**0.9**
$7C_3$	7-26	00:48-01:06	CLR	6.0	**0.9**
$7C_4$	7-26	01:06-01:20	CLR	6.0	**1.5**
$7C_5$	7-26	01:20-01:35	CLR	6.0	**1.0**
$7C_6$	7-26	01:35-01:48	CLR	6.0	**0.7**

The downtown-to-Lake Draper route was driven five times during the experiment. Figure 3 shows temperature measurements obtained over this route between 2:32 am and 3:18 am (CDT) on July 19, 2003. As on other nights, the temperatures are warmest in the downtown area and are coolest in the rural areas adjacent to the Lake. During this route, the temperature difference between the urban core and the rural area is about 5.2°C. As shown in Table 4, the urban-rural ΔT for this route varied from 5.5°C to 6.5°C during the experiment. Even though winds were moderate, larger ΔT's were measured on this route as compared to the other routes, perhaps indicative of cooler rural temperatures measured at this location. For example, on the night of July 18 at around 3 am the ΔT measured on this route was between 5.5 and 6.5°C, while at 3:30 am on the Downtown-to-Airport route it was only around 2°C.

Table 4 – Urban-Rural Temp. Difference Downtown-L. Draper Route

Expt No.	Date	Time (CDT)	Cloud Cover	wind speed (m/s)	ΔT (C)
$3D_1$	7-18	02:32-02:52	CLR	4.0	**5.4**
$3D_2$	7-18	02:52-03:18	CLR	4.0	**6.4**
$4A_1$	7-18	23:38-23:57	CLR	4.0-4.5	**5.4**
$6B_1$	7-21	22:54-23:15	CLR	5.0	**5.4**
$6B_2$	7-21	23:15-23:43	CLR	5.0	**6.2**

The last primary route driven during the experiment was the downtown-to-east rural route, which was driven nine times. This route went east from the downtown core to a large undeveloped vegetated area near a gravel plant. Figure 4 shows temperature measurements obtained over this route between 11:16 pm and 11:25 pm (CDT) on July 25, 2003. As on other nights, the temperatures are warmest in the downtown area and are coolest in the rural areas, with intermediate temperatures in the residential and wooded area in between. During this route, the temperature difference between the urban core and the rural area is only about 0.7°C. As shown in Table 5, the urban-rural ΔT for this route varied from 0.5°C to 1.0°C during the experiment with one outlier of about 4°C. On July 25th, the route was driven 7 times in a row. The variability in the measured ΔT over this relatively short route gives some estimate of the uncertainty in the measurements. The small ΔT measured on this night agrees with the values from the Downtown-to-NE Lake route driven on this same night.

Table 5 – Urban-Rural Temp. Difference Downtown-East Rural Route

Expt No.	Date	Time (CDT)	Cloud Cover	wind speed (m/s)	ΔT (C)
$5B_1$	7-19	23:51-23:59	SCT 230	5.5	**3.8**
$7B_2$	7-25	22:38-22:47	CLR	5.0	**0.6**
$7B_3$	7-25	22:47-22:56	CLR	5.5-6.0	**0.9**
$7B_4$	7-25	22:56-23:08	CLR	5.5-6.0	**0.7**
$7B_5$	7-25	23:06-23:16	CLR	5.5-6.0	**1.1**
$7B_6$	7-25	23:16-23:25	CLR	5.5-6.0	**0.7**
$7B_7$	7-25	23:25-23:34	CLR	5.5-6.0	**1.1**
$7B_8$	7-25	23:34-23:44	CLR	5.5-6.0	**0.8**

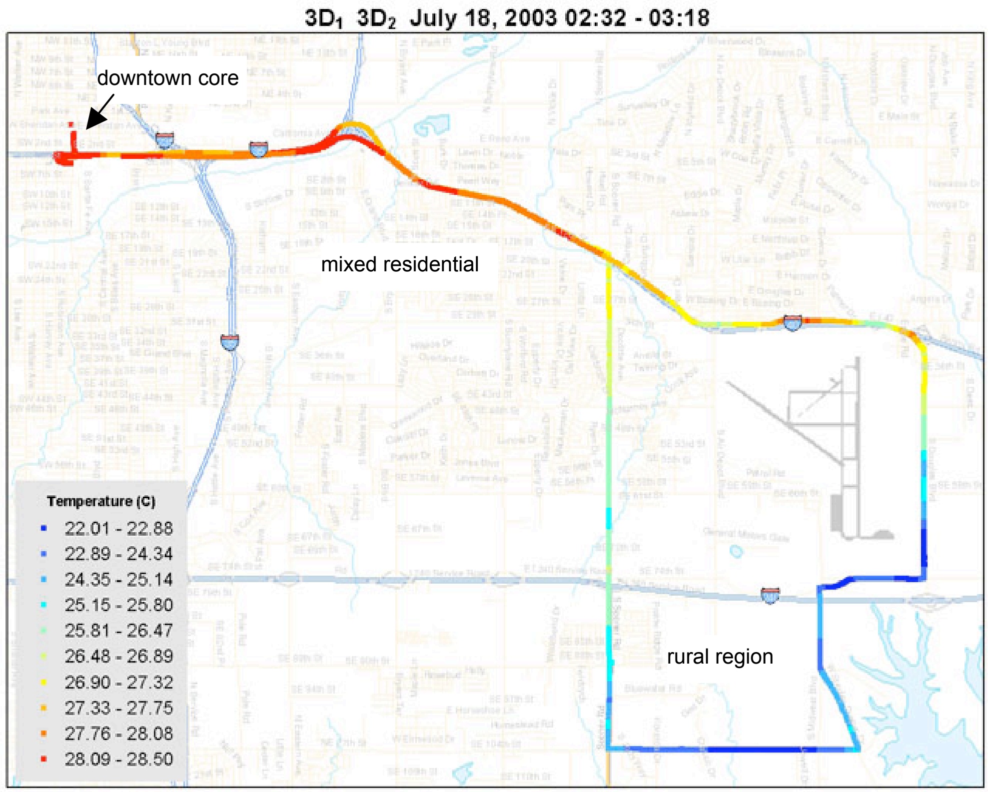

Figure 3. The downtown-to-Lake Draper route showing temperature measurements made at 2.5 m above ground level in the early morning hours of July 18, 2003.

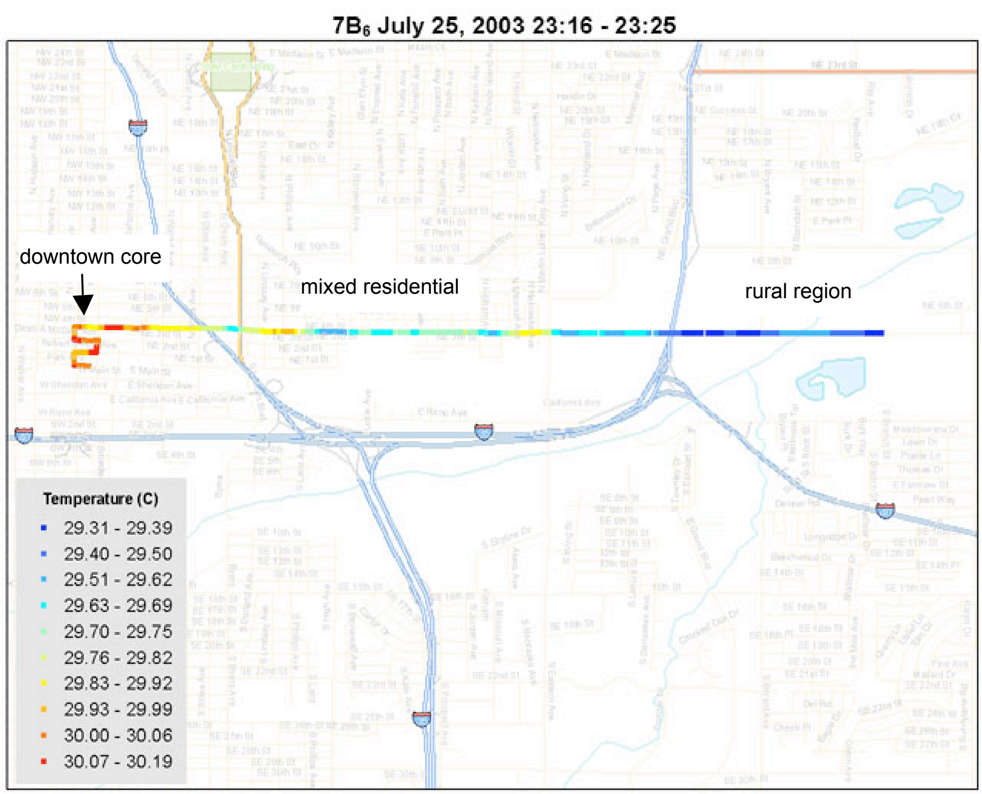

Figure 4. The downtown-to-Rural Gravel Plant route showing temperature measurements made at 2.5 m above ground level on the night of July 25, 2003.

4.2 Remote Sensing

After requesting more than fifty images from the LPDAAC, a daytime image captured on July 21, 2001 at 17:27 CDT was chosen for analysis because it is cloud-free and covers our region of interest (ROI) completely (Fig. 5). We were not able to obtain a viable image for the period of the Joint Urban 2003 Field Experiment.

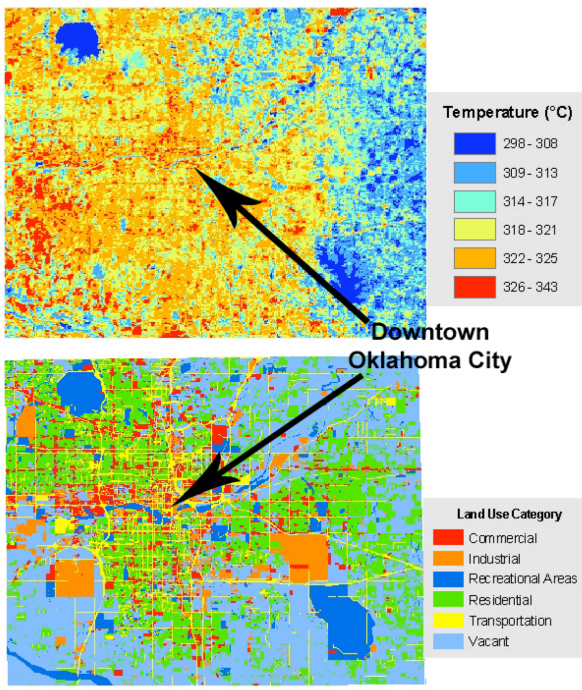

Figure 5. July 21, 2001 ASTER skin temperature image of OKC area at 17:21 CDT and Land Use map of the OKC area.

Figure 5 shows our ROI which encompasses the entire Oklahoma City urban corridor and various residential and rural areas. Significant variations in skin temperature across the ROI are evident. For example, the relatively cool hydrological features such as Lake Hefner (Northwest ROI) and Lake Stanley Draper (Southeast ROI) are particularly easy to distinguish. Of additional note is the area to the southwest of downtown OKC where skin temperatures approach 340°K. Using the landuse map shown above, this region of very warm temperatures is associated with a large industrial area.

Both the ASTER image and the ACOG land use data were geographically projected within ArcGIS to perform a land use-temperature correlation analysis. Using the zonal statistics function of ArcGIS we calculated the median skin temperature within the six land use categories as defined in Table 6.

Table 6. Land Use Description

Land Use Category	Description
Recreational Areas	Parks, open spaces, lakes, waterways
Vacant & Agriculture	Active/passive agricultural, vacant, Farmsteads
Residential	Rural residential, urban single/multiple family, mobile home parks
Transportation	Railroad, roads, arterial right-of-way
Industrial	Warehousing, transportation and utilities, mineral extraction, land fill, water treatment plant
Commercial	Public & private office setting, malls, state capitol complex, schools, hospitals, colleges

Source: ACOG, 1995

Figure 6 shows that the median daytime skin temperature for urban areas is warmer than non-urban areas in our ROI. Minor temperature differences are found among the urban industrial, commercial, and transportation land use categories. Residential and agricultural skin temperature was approximately 1.5°K and 2.5°K cooler than these urban areas, respectively, while recreational areas were nearly 8°K cooler. These temperature differences can be attributed to the physical differences in thermal properties between the aforementioned land use categories. Recreational areas such as parks and open spaces are primarily undeveloped with vegetation and water bodies, the agricultural areas are predominately vegetated, residential areas have a mix of developed areas and vegetated areas, whereas industrial and commercial areas are usually more developed, comprised of heat absorbing surfaces and structures, and contain less vegetation in general.

To better understand the variability within each land use category we have examined the standard deviation about the median of the skin temperatures for each land use category. Table 7 shows the standard deviation in °K of each land use category. Recreational areas and vacant & agriculture land use categories have the highest standard deviations. The 8.04°K standard deviation for recreational areas can be attributed to the inclusion of waterways and lakes in this category.

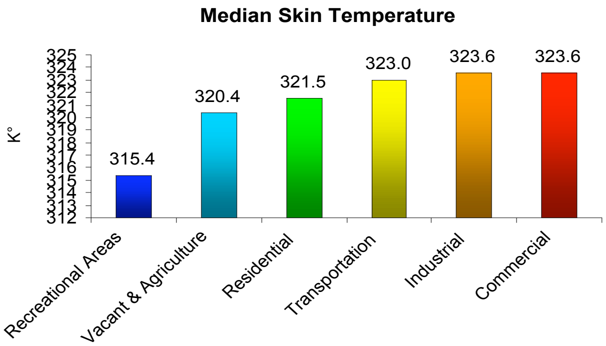

Figure 6. Median Skin Temperature by Land Use.

Table 7: Standard Deviation of Median Skin Temperature

Land Use Category	Standard Deviation
Recreational Areas	8.04°K
Vacant & Agriculture	5.57°K
Residential	4.33°K
Transportation	4.24°K
Industrial	3.84°K
Commercial	3.67°K

These hydrological features are considerably cooler than the surrounding land surfaces and contribute to a large spread about the median skin temperature for this category. It is also interesting to note that the industrial and commercial land use categories have the smallest standard deviations of 3.84°K and 3.67°K respectively. The reason the developed urban areas have a smaller range in skin temperatures may be because they are primarily composed of man-made surfaces with similar thermal properties.

5. SUMMARY

Ground measurements and a remotely sensed image were analyzed in order to investigate the urban heat island phenomenon in Oklahoma City. Ground measurements of air temperature show distinct temperature differences between urban and rural areas on different days and in variable weather conditions. Additionally, the temperature difference between rural and urban areas varied significantly depending upon the route chosen. For example, urban-rural air temperature differences for the Downtown-to-Lake Draper route were often more pronounced than those observed on the Downtown-NE Lake route.

As expected, analysis of the remotely sensed ASTER image indicates significantly warmer skin temperatures in urban areas as compared to non-urban areas during the daytime. Note that this is not indicative of a daytime urban heat island because these are not air temperatures. Nonetheless, analysis of this image does provide further insight into skin temperature differences that can be associated with daytime heating in developed, urban areas which will then impact the development of the nighttime urban heat island.

Future work will include comparison to PNNL HOBO temperature data and temperature measurements from a large number of meteorological stations placed around Oklahoma City. In addition, measurements will be correlated not only to land use, but to population and building density. Finally, we will further investigate the impact of wind speed and direction on heat island intensity and compare to the results of other experiments (e.g., Oke, 1987).

6. REFERENCES

Allwine, J., K. Clawson, M. Leach, D. Burrows, R. Wayson, J. Flaherty, and E. Allwine, 2004: Urban dispersion processes investigated during the Joint Urban 2003 study in Oklahoma City, 5th AMS Urban Env. Conf., Vancouver, B.C.

Chin, H.N., M.J. Leach, and M.J. Brown, 2000: A Sensitivity Study of the Urban Effect on a Regional-Scale Model: An Idealized Case, 3rd AMS Urban Env. Symp., Davis, CA.

Holt, T. and J.J. Shi, 2004: Mesoscale simulations of the urban environment of Washington, D.C.: Comparison of COAMPS simulations to DCNET observations and sensitivity of plume transport to an urban canopy parameterization. Paper 4.3, Symp. on the Urban Zone, 84th Annual AMS Meeting, Seattle, WA.

Oke, T., 1987: *Boundary-Layer Climates*, Routledge, London.